

# Regular and Irregular Mixing in Blends of Saturated Hydrocarbon Polymers

William W. Graessley,\* Ramanan Krishnamoorti,<sup>†</sup> and Glenn C. Reichart

Department of Chemical Engineering, Princeton University, Princeton, New Jersey 08544

Nitash P. Balsara,<sup>‡</sup> Lewis J. Fetters, and David J. Lohse

Corporate Research Laboratories, Exxon Research and Engineering Company, Annandale, New Jersey 08801

Received June 24, 1994; Revised Manuscript Received November 21, 1994\*

**ABSTRACT:** Thermodynamic interactions in binary blends of model polyolefins were investigated by small-angle neutron scattering (SANS), cloud-point determinations, and PVT measurements. Results for four microstructures—atactic polypropylene, head-to-head polypropylene, and two saturated samples of polyisoprenes with reduced 1,4 content—were incorporated into a solubility parameter (SP) scheme that had been developed earlier for various model copolymers of ethylene with propylene and 1-butene. Component SP values were assigned, after confirming their uniqueness by various tests of internal consistency, with SANS-determined interaction strengths for their blends with other components. As found earlier, the SANS-based assignments agree rather well with independent estimates of SP from the pure component PVT properties. Several new instances of irregular mixing—blends for which the interaction strength departs significantly from the SP prediction—were identified, and some apparent patterns were noted. The suggested relationship between interaction strength and mismatch of component segment lengths was also examined in some detail. What we find is an interesting global correlation between segment length and SP assignment, whether obtained from SANS data or inferred from pure component PVT properties, but no connection at all between segment length mismatch in blends and either the temperature dependence of interaction strength or the presence of mixing irregularity.

## Introduction

This paper is one of a series on the thermodynamic interactions in melt-state blends of saturated hydrocarbon polymers. The components are model polyolefins, made by saturating the double bonds in nearly monodisperse polydienes with either H<sub>2</sub> or D<sub>2</sub>. The small-angle neutron scattering (SANS) and light scattering procedures we use as described in the first paper of the series.<sup>1</sup> Another<sup>2</sup> describes the measurement of equation-of-state (PVT) properties for individual components. Subsequent papers have dealt with effects of deuteration,<sup>3-5</sup> blend composition,<sup>6</sup> and component microstructures<sup>7,8</sup> on values of the Flory-Huggins parameter  $\chi$ , as obtained by SANS.

For numerous blends of these polymers—hydrogenated polybutadienes (HPB; model statistical copolymers of ethylene and 1-butene), hydrogenated 1,4-polyisoprene (PEP; a model alternating copolymer of ethylene and propylene), and hydrogenated 1,4-poly(ethylbutadiene) (PEB; a model alternating copolymer of ethylene and 1-butene)—we have shown that the values of  $\chi$  can be organized in the framework of a regular solution theory, expressed in terms of the Hildebrand equation:<sup>9</sup>

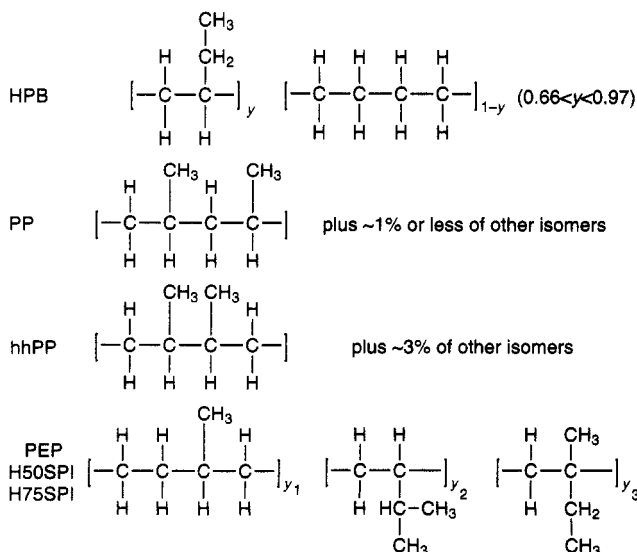
$$\chi = \frac{v_0}{k_B T} (\delta_2 - \delta_1)^2 \quad (1)$$

where  $v_0$  is the reference volume for  $\chi$  and  $\delta_1$  and  $\delta_2$  are empirically-assigned, temperature-dependent solubility parameters for species 1 and 2.<sup>8</sup> In only one of the 10 blends investigated was there a clear indication of departure in  $\chi$  from internal consistency with uniqueness in the assigned values of  $\delta(T)$  for each species. We have also shown that the differences in component solubility parameters deduced from the SANS data are in reasonable accord with those inferred independently from PVT measurements on the components.<sup>7,8</sup> Here

we report results for 13 new blends that include components with four other microstructures—atactic polypropylene (PP), atactic head-to-head polypropylene (hhPP), and two hydrogenated polyisoprenes with reduced 1,4 content (50SPI and 75SPI). Among these blends we find several more in which  $\chi$  clearly departs from the solubility parameter formalism. We also provide further comparisons of SANS-based and PVT-based assignments of the solubility parameter. Finally, we explore in some detail the recent suggestion that the interactions in polyolefin blends are primarily entropic and originate from a mismatch in the component statistical segment lengths.

## Experimental Section

The chemical microstructures of the components in this study originate from the various modes of enchainment of butadiene (the HPB series), 2-methylpentadiene (PP), 2,3-dimethylbutadiene (hhPP), and isoprene (PEP, 50SPI, 75SPI). The polydiene precursors were catalytically saturated with either H<sub>2</sub> or D<sub>2</sub>, as described previously.<sup>1</sup> The fully hydrogenous versions contain the following microstructural units:



\* Present address: Department of Chemical Engineering, California Institute of Technology, Pasadena, CA 91125.

<sup>†</sup> Present address: Department of Chemical Engineering, Polytechnic University, Brooklyn, NY 11201.

<sup>‡</sup> Abstract published in *Advance ACS Abstracts*, February 1, 1995.

Table 1. Molecular Characterization of Blend Components

sample	degree of polymn <i>N</i>	carbon atoms per monomeric unit	density at 23.0 °C $\rho_H$ (g/cm <sup>3</sup> )	glass transition temp $T_g$ (°C)	deuterium atoms per monomeric unit
H97A (D97A)	1600	4	0.8658	-22	2.79
H97B (D97B)	865	4	0.8651	-25	2.69
H88 (D88)	1610	4	0.8642	-34	2.96
H78 (D78)	1285	4	0.8630	-45	2.37
H66 (D66)	2040	4	0.8635	-54	3.25
HPEP (DPEP)	855	5	0.8539	-59	4.70
HPEB (DPEB)	550	5	0.8636	-55	3.18
H50PI (D50SPI)	1485	5	0.8630	-22	4.66
H75PI (D75SPI)	1010	5	0.8878	+19	4.50
HhhPPA (DhhPPA) <sup>a</sup>	320	6	0.8726	-24	3.97
HhhPPB (DhhPPB)	910	6	0.8736	-24	4.10
HhhPPC (DhhPPC)	2045	6	0.8726	-20	5.16
HPPA (DPPA)	130	6	0.8504	-1	4.24
HPPB (DPPB)	705	6	0.8629	+1	3.88

<sup>a</sup> The sample hhPPA was designated hhPP in ref 5.

Table 2. Selected Component PVT Properties

sample	<i>T</i> (°C)	$\alpha(T) \times 10^4$ (K <sup>-1</sup> )	$\beta(T) \times 10^4$ (MPa <sup>-1</sup> )	$\delta(T)$ (MPa <sup>1/2</sup> )
HPP	27	7.2 <sub>8</sub>	6.4 <sub>7</sub>	18.3 <sub>7</sub>
	51	7.5 <sub>5</sub>	7.5 <sub>4</sub>	18.0 <sub>2</sub>
	83	7.3 <sub>1</sub>	8.7 <sub>3</sub>	17.2 <sub>5</sub>
	121	7.3 <sub>0</sub>	10.4 <sub>4</sub>	16.6 <sub>0</sub>
	167	7.5 <sub>2</sub>	13.1 <sub>4</sub>	15.8 <sub>7</sub>
HhhPP	27	6.7 <sub>0</sub>	5.6 <sub>9</sub>	18.8 <sub>0</sub>
	51	6.9 <sub>2</sub>	6.6 <sub>0</sub>	18.4 <sub>5</sub>
	83	6.8 <sub>1</sub>	7.6 <sub>0</sub>	17.8 <sub>5</sub>
	121	7.0 <sub>2</sub>	9.0 <sub>1</sub>	17.5 <sub>2</sub>
	167	7.1 <sub>5</sub>	11.3 <sub>0</sub>	16.6 <sub>8</sub>
H50SPI	27	6.8 <sub>9</sub>	5.9 <sub>7</sub>	18.6 <sub>2</sub>
	51	7.1 <sub>2</sub>	6.9 <sub>4</sub>	18.2 <sub>4</sub>
	83	6.9 <sub>2</sub>	8.0 <sub>7</sub>	17.4 <sub>6</sub>
	121	7.1 <sub>0</sub>	9.6 <sub>8</sub>	17.0 <sub>0</sub>
	167	7.4 <sub>5</sub>	11.9 <sub>7</sub>	16.5 <sub>4</sub>

Following previous conventions,<sup>1</sup> the microstructure code (100y for members of the HPB series and PP, PEP, etc., for the others) is sandwiched between an initial "H" or "D", distinguishing the fully hydrogenous and partially deuterated versions, and a final "A", "B", etc., when two or more samples with the same microstructure but different molecular weight were used. The various saturated polyisoprenes have different proportions of monomeric 1,4 ( $y_1$ ), 3,4 ( $y_2$ ), and 1,2 ( $y_3$ ) enchainment—for PEP,  $y_1 = 0.93$ ,  $y_2 = 0.07$ ,  $y_3 = \sim 0$ ; for 50SPI,  $y_1 = 0.50$ ,  $y_2 = 0.50$ ,  $y_3 = \sim 0$ ; and for 75SPI,  $y_1 = \sim 0$ ,  $y_2 = 0.75$ ,  $y_3 = 0.25$ . Polymers with essentially identical microstructures have been studied in dilute solution (good solvents and at the  $\Theta$ -condition).<sup>10</sup> (The H50SPI and H75SPI samples are H50PI80 and H34PI65 in the earlier study by Mays et al.<sup>10a</sup> From NMR, the sequencing of units is nearly random, and the microstructures are atactic. All samples in this study are noncrystalline. Their molecular and physical characteristics, obtained as described elsewhere,<sup>1</sup> are listed in Table 1.

The PVT properties of selected components were measured with the Zoller apparatus (Gnomix, Inc.) by procedures that are explained elsewhere.<sup>2</sup> The data were provided through the courtesy of Dr. Gregory T. Dee of Dupont Central Research and Development. The low-pressure limits of thermal expansion coefficient  $\alpha$  and isothermal compressibility  $\beta$  at several temperatures are listed in Table 2.

The SANS measurements were made at the NIST Cold Neutron Research Facility in Gaithersburg, MD.<sup>1,11</sup> Scattering profiles for blends of hydrogenous and deuterated components were obtained on the 8-m beamline (NG5). By methods explained elsewhere,<sup>1</sup> the data were analyzed through the incompressible random-phase approximation as applied to the Flory-Huggins (FH) expression for mixing free energy. Interaction strength was expressed in terms of the FH interaction parameter  $\chi$ , defined with respect to the arbitrary reference volume  $v_0 = [v_1(T) v_2(T)]^{1/2}$ , where  $v_1$  and  $v_2$  are volumes per mer for the components. Unless otherwise stated, the values of  $\chi$  were obtained in the midrange of blend

composition:  $\phi_1 \sim \phi_2 \sim 0.5$ , where the  $\phi_i$ 's are component volume fractions. The estimated systematic uncertainties in  $\chi$  are  $\pm 1.5 \times 10^{-4}$ .<sup>1</sup> The results for matched pair mixtures<sup>1</sup> provided the radius of gyration  $R_g$  and the nominal isotopic interaction parameter ( $\chi_{HD}$ )<sub>apparent</sub> for each component.<sup>1</sup> Values not already reported elsewhere are listed in Table 3. Interaction parameters for the blends are listed in Table 4. Results obtained with different labeling configurations or molecular weights for the same pair of microstructures are grouped together.

## Survey of Results

The miscibility of 50SPI with a wide variety of model polyolefin components was surveyed by light scattering.<sup>12</sup> Single-phase blends were obtained over most of the available temperature range (27 °C  $\leq T \leq$  167 °C) only with 78, 88, and hhPPA as second components, although the 50SPI/PPB blends were also single phase above 100 °C. The SANS data for 50SPI/88 and 50SPI/hhPPA (Table 4) are unremarkable, exhibiting UCST behavior with  $\chi(T)$  obeying the conventional  $A/T + B$  form. The interactions in 50SPI/78, on the other hand, are extremely weak and insensitive to temperature, as shown in Figure 1. Among all the blends we have studied, these are the nearest to being ideal mixtures over the entire 27–167 °C range. The matched pair mixtures have interaction strengths in this range (see Table 3), but even ( $\chi_{HD}$ )<sub>apparent</sub> varies more strongly with temperature than  $\chi_{78/50SPI}$ . The negative signs indicate a weak attraction between components. There is also a label-switching effect<sup>3</sup> that we find in nearly all our blends.<sup>3,5</sup>

The blends of 75SPI and 97 were found to be single phase over the entire temperature range. The SANS data indicate rather modest interaction strengths (Table 4), UCST behavior, and conventional  $\chi(T)$  behavior.<sup>12</sup> From light scattering, the three forms of saturated polyisoprene (PEP, 50SPI, 75SPI) were mutually immiscible, even far away from the critical composition and at high temperatures.<sup>12</sup>

The two polypropylene microstructures, PP and hhPP, exhibit markedly different mixing behavior in blends with other model polyolefins. Thus, for example, hhPP is miscible with PEP, PEB, and 66 up to very high molecular weights, while only the lowest molecular weight PP (PPA;  $N = 130$ ) is miscible with PEP. (Blends of PPA with PEB and 66 were not investigated.) Also, PP is miscible with 97,<sup>13</sup> yet hhPP is already immiscible even with 90.<sup>12</sup> The blends of PP with hhPP have large interaction parameters, as shown in Figure 2. Again, however, the temperature dependence is conventional.

**Table 3. Chain Dimensions and Apparent Isotopic Interaction Parameter from SANS Results for Matched Pair Mixtures**

matched pair	27 °C		51 °C		83 °C		121 °C		167 °C	
	$R_g$ (Å)	$(\chi_{HD})_{apparent} \times 10^4$	$R_g$ (Å)	$(\chi_{HD})_{apparent} \times 10^4$	$R_g$ (Å)	$(\chi_{HD})_{apparent} \times 10^4$	$R_g$ (Å)	$(\chi_{HD})_{apparent} \times 10^4$	$R_g$ (Å)	$(\chi_{HD})_{apparent} \times 10^4$
H50SPI/D50SPI	105.4	-0.5	104.5	-1.1	104.4	-1.5	105.0	-2.1	104.5	-2.4
H75SPI/D75SPI	73.3	2.5	73.9	2.4	74.9	1.7	76.4	0.7	79.2	-0.3
HhhPPA/DhhPPA	55.5	5.7	56.1	4.4	56.1	2.1	56.2	0.1	56.4	-1.4
HhhPPPB/DhhPPB	94.2	2.5	94.4	2.1	94.1	1.4	94.1	1.0	94.4	0.7
HhhPPC/DhhPPC	139.7	2.7	139.7	1.9	139.2	1.3	139.4	1.0	140.2	0.7
HPPA/DPPA <sup>a</sup>	35.3		34.5		34.2		34.1			
HPPB/DPPB	78.8	1.9	79.2	1.6	79.6	1.4	79.9	1.2	80.3	0.9

<sup>a</sup> The wormlike chain model was used to evaluate  $R_g$  for PPA, owing to its low molecular weight,<sup>12</sup> and  $(\chi_{HD})_{apparent}$  could not be evaluated.

**Table 4. Interaction Parameters vs Temperature for Blends**

blend <sup>a</sup>	$\chi \times 10^4$ at temp $T$ (°C)									
	27	51	83	98	108	121	138	143	167	
H50SPI/DhhPPA	29.4	24.0	19.1			14.1			11.2	$\delta_{hhPP} > \delta_{50SPI}$
D50SPI/HhhPPA	two phases	33.2	29.9			24.1			19.3	
H50SPI/D88	two phases	two phases		10.3		8.9		8.0	6.8	$\delta_{50SPI} > \delta_{88}$
D50SPI/H88	11.3	10.0		7.8		6.7		5.8	4.9	
H50SPI/D78	-3.6	-3.7	-3.5				-3.5		-3.4	?
D50SPI/H78	-1.0	-1.2				-1.0	-1.2		-1.8	
H75SPI/D97B	8.4	7.6	6.9			6.0			5.0	$\delta_{97} > \delta_{75SPI}(?)$
D75SPI/H97B	9.0	8.3	7.3				6.5			
D75SPI/HPPA	60.6	51.5	44.4							
HhhPPA/DPPA	46.5	37.5	29.0			20.0				$\delta_{hhPP} > \delta_{PP}$
DhhPPA/HPPA	35.5	27.5	22.5			16.0				
HhhPPA/D78	two phases				24.2		21.2		18.8	$\delta_{hhPP} > \delta_{78}$
DhhPPA/H78	33.2	28.2	23.1		20.4		17.2		14.8	
HhhPPA/D66	19.5	11.6	5.6			1.8			0.9	
DhhPPA/H66	19.9	12.2	6.3			2.4			1.4	?
DhhPPB/H66	19.1	11.7	5.4			1.5			0.6	
HPEB/DhhPPA	20.7	17.2	13.9			11.2			10.2	
DPEB/HhhPPA	19.4	16.7	13.5			11.1			10.0	?
DPEB/HhhPPB	18.2	15.7	12.5			10.1			9.0	
HPEP/DhhPPA	15.4	11.5	9.2			8.4			10.0	
DPEP/HhhPPA	6.1	2.6	0.5			1.1			3.2	$\delta_{PEP} > \delta_{hhPP}$
DPEP/HhhPPB	9.1	6.0	3.8			5.1			6.9	
DPEP/HhhPPC	9.7	5.9	3.7			5.7			7.6	
HPEP/DhhPPC	two phases	two phases	15.2			15.8			16.4	
H97A/DPPA	42.5	31.5	21.5			12.5				
D97A/HPPA	53.0	40.0	28.5			19.5				$\delta_{PP} > \delta_{97}$
D97B/HPPA <sup>b</sup>	50.5	41.5	32.5			22.0				
HPPB/D78	two phases	18.1	11.1			6.2			4.9	$\delta_{78} > \delta_{PP}$
DPPB/H78	two phases	20.7	14.7			9.6			7.2	
HPEP/DPPA <sup>c</sup>	49.5	53.0	56.5			56.5			55.5	
DPEP/HPPA <sup>d</sup>	27.5	32.5	38.5			41.5			42.5	$\delta_{PEP} > \delta_{PP}$
DPEP/HPPA <sup>e</sup>	34.5	36.5	41.5			46.0			47.0	

<sup>a</sup> All blends near the concentration midrange ( $\phi_1 = \phi_2 = 0.5 \pm 0.03$ ) unless stated otherwise. <sup>b</sup>  $\phi(\text{HPPA}) = 0.81_6$ ; D97A/HPPB (at  $\phi \sim 0.50$ ) is two-phase up to 200 °C. <sup>c</sup>  $\phi(\text{DPPA}) = 0.69_3$ , chosen to be near the critical composition. <sup>d</sup>  $\phi(\text{HPPA}) = 0.70_1$ , chosen to be near the critical composition. <sup>e</sup>  $\phi(\text{HPPA}) = 0.87_2$ .

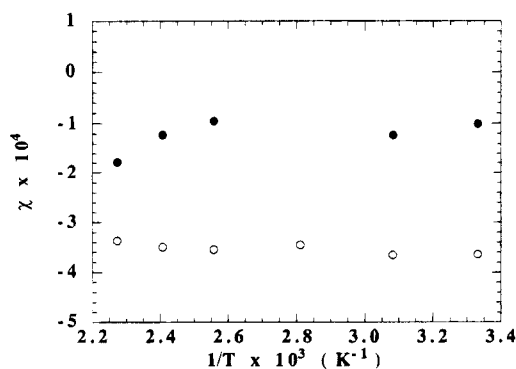


**Figure 1.** Temperature dependence of  $\chi$  for 50SPI/78 blends. The symbols indicate the H50SPI/D78 blend (○) and the D50SPI/H78 blend (●).

The interaction parameter for PEP/hhPPA blends is shown in Figure 3. The interaction strength is only moderate, and the effect of label-switching is large, but

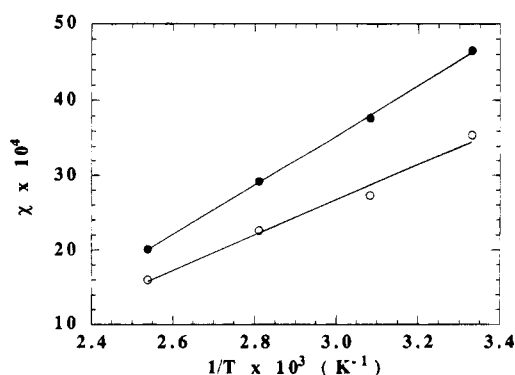


**Figure 2.** Temperature dependence of  $\chi$  for hhPPA/PPA blends. The symbols indicate HhhPPA/DPPA (●) and DhhPPA/HPPA (○).

the most interesting feature is the temperature dependence. The intermediate minimum in  $\chi(T)$ , also observed for DPEP/HhhPPB, HPEP/DhhPPC, and DPEP/

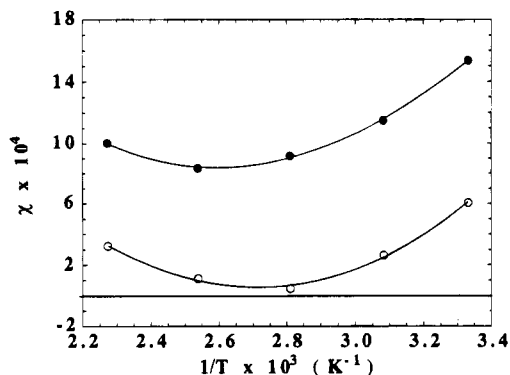


**Figure 3.** Temperature dependence of  $\chi$  for PEP/hhPPA blends. The symbols indicate HPEP/DhhPPA (●) and DPEP/hhPPA (○).

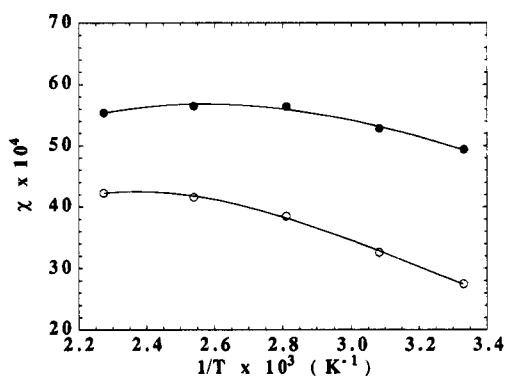


**Figure 4.** Temperature dependence of  $\chi$  for PEP/PPA blends. The symbols indicate HPEP/DPPA (●) and DPEP/HPPA (○).

HhPPC (see Table 4), suggests the possibility of both LCST and UCST behavior in PEP/hhPP blends.

The SANS results for PEP/PPA blends are shown in Figure 4. The interaction in this case is very large, and its temperature dependence suggests LCST behavior. Lohse et al.<sup>14</sup> recently estimated  $\chi_{PP/PEP} = 35 \times 10^{-4}$  at room temperature from thermal analyses of both diblocks and blends of HPP and HPEP. The SANS value at 27 °C, corrected for the isotope effect,<sup>3,5</sup> is  $38 \times 10^{-4}$ .

## Discussion

**A. Effect of Chain Length on Interaction Strength.** Over the course of this and earlier investigations we have evaluated  $\chi(T)$  for the same pair of microstructures but different component molecular weights. Those results, reviewed in Appendix A, indicate that chain length effects are small and in all cases (with the possible exception of the hhPP/PEP blends) within the uncertainties of the data. That conclusion, and the agreement noted above in  $\chi_{PP/PEP}$  for blends and diblocks, supports the supposition that interaction strength in blends of saturated hydrocarbon polymers is locally determined and therefore insensitive to the global features of structure if the chains are long.

**B. Solubility Parameter Formulation.** We have found that eq 1 serves as a useful organizing principle for the interactions in many blends of saturated hydrocarbon polymers. With one of the components as an arbitrary reference we found that unique values of  $\delta - \delta_{\text{ref}}$  could be assigned to PEP, PEB, and several HPB components from the values of  $\chi$  for a highly interconnected set of their blends.<sup>8</sup> Uniqueness was established in the following way. Tentative values  $(\delta_2 - \delta_1)'$  were calculated from  $\chi$  for each blend and temperature with eq 1, its sign being inferred from the direction of the

label-switching effect.<sup>3,5</sup> Uniqueness for an  $\alpha/\beta$  blend, for example, was tested with the results from other blends of species  $\alpha$  and  $\beta$  with, for example, some third component  $\gamma$ —the  $\alpha/\gamma$  and  $\beta/\gamma$  blends. Consistency with the solubility parameter formalism requires

$$(\delta_\beta - \delta_\alpha)' = (\delta_\beta - \delta_\gamma)' - (\delta_\alpha - \delta_\gamma)' \quad (2)$$

The left side represents the *direct tentative* value for the difference in solubility parameters for species  $\alpha$  and  $\beta$ , and the right side represents an *indirect tentative* value. Blends that are consistent with eq 2 (within some error bounds) are called *regular mixtures*. Confirmed values of  $\delta - \delta_{\text{ref}}$  for their components can then be obtained by applying eq 2 through a connected sequence of *regular mixtures* to reach the reference component. Inconsistency with eq 2 means that one or more blends in the connected sequence— $\alpha/\beta$ ,  $\alpha/\gamma$ ,  $\beta/\gamma$  in the example—are *irregular mixtures*. Other closed-loop sequences must then be used to identify which of these blends mix irregularly and to assign values of  $\delta - \delta_{\text{ref}}$  for their components.

Such procedures work best of course when many independent tests of internal consistency are applied and when most blends mix regularly. Nine of the ten blends in the previous study (omitting isotopic differences) displayed regular mixing at all temperatures with several cross-checks.<sup>8</sup> Only the 66/PEB blends were irregular. The indirect tentative values from blends of 66 and PEB with various third components agreed, but the direct tentative values (from the 66/PEB blend itself) were clearly different.

Similar procedures for distinguishing regular and irregular mixing, and for assigning values of  $\delta - \delta_{\text{ref}}$ , were applied to the blends in this work. These include the blends involving hhPP that had been shown earlier to be qualitatively inconsistent with solubility parameter uniqueness.<sup>5</sup> The last column in Table 4 shows the ordering of  $\delta$  inferred from the effect of label-switching. These orderings are based on the supposition that the solubility parameter of any saturated hydrocarbon is reduced by deuterium substitution,<sup>3</sup> leading to an increase in the magnitude of  $\delta_2 - \delta_1$  (and therefore  $\chi$ , from eq 1) when the component with the lower solubility parameter is deuterated. Switching the deuterium labels decreases  $\chi$ , and, for comparable labeling levels, fair estimates for the unlabeled and doubly labeled versions are averages of singly labeled values:<sup>3</sup>

$$\chi_{hh}^{1/2} = \chi_{dd}^{1/2} = \frac{\chi_{hd}^{1/2} + \chi_{dh}^{1/2}}{2} \quad (3)$$

$$(\delta_2 - \delta_1)_{hh} = (\delta_2 - \delta_1)_{dd} = \frac{(\delta_2 - \delta_1)_{hd} + (\delta_2 - \delta_1)_{dh}}{2} \quad (4)$$

We have used these equations extensively in earlier work<sup>5,7,8</sup> to estimate  $\chi_{hh}$  from SANS data for  $\chi_{hd}$  and  $\chi_{dh}$ .

From the orderings of  $\delta$  in Table 4 we obtain the following relationships over the observed temperature range:

$$\begin{aligned} \delta_{\text{PEP}} &> \delta_{\text{hhPP}} > \delta_{78} \\ \delta_{78} &> \delta_{\text{PP}} > \delta_{97} \\ \delta_{\text{hhPP}} &> \delta_{50\text{SPI}} > \delta_{88} \end{aligned} \quad (5)$$

The ordering  $\delta_{52} \sim \delta_{\text{PEP}} > \delta_{66} \sim \delta_{\text{PEB}} > \delta_{78} > \delta_{88} > \delta_{97}$

Table 5. Direct and Indirect Tentative Values

sequence	27 °C	51 °C	83 °C	121 °C	167 °C
a. Direct and Indirect Tentative Values of $\delta_{\text{HPEP}} - \delta_{\text{DhhPPA}}$ and $\delta_{\text{DPEP}} - \delta_{\text{HhhPPA}}$					
$(\delta_{\text{HPEP}} - \delta_{\text{DhhPPA}})' (\text{MPa})^{1/2}$					
direct measurement	0.20 <sub>7</sub>	0.18 <sub>5</sub>	0.17 <sub>1</sub>	0.17 <sub>0</sub>	0.19 <sub>3</sub>
HPEP-D66-H78-DhhPPA	0.12 <sub>5</sub>	0.14 <sub>4</sub>	0.16 <sub>5</sub>	0.18 <sub>0</sub>	0.19 <sub>8</sub>
HPEP-DPEP-H78-DhhPPA	0.11 <sub>1</sub>	0.12 <sub>7</sub>	0.14 <sub>7</sub>	0.17 <sub>0</sub>	0.19 <sub>3</sub>
$(\delta_{\text{DPEP}} - \delta_{\text{HhhPPA}})' (\text{MPa})^{1/2}$					
direct measurement	0.13 <sub>0</sub>	0.08 <sub>9</sub>	0.03 <sub>9</sub>	0.06 <sub>2</sub>	0.11 <sub>0</sub>
DPEP-H66-D78-HhhPPA	0.08 <sub>9</sub>	0.10 <sub>0</sub>	0.11 <sub>7</sub>	0.13 <sub>7</sub>	0.15 <sub>5</sub>
DPEP-HPEB-D78-HhhPPA	0.13 <sub>1</sub>	0.13 <sub>6</sub>	0.14 <sub>5</sub>	0.16 <sub>0</sub>	0.17 <sub>8</sub>
b. Direct and Indirect Tentative Values of $\delta_{\text{H66}} - \delta_{\text{HhhPPA}}$ and $\delta_{\text{HPEB}} - \delta_{\text{HhhPPA}}$					
$(\delta_{\text{H66}} - \delta_{\text{HhhPPA}})' (\text{MPa})^{1/2}$					
direct measurement	0.25	0.20	0.15	0.09	0.07
66-78-hhPPA; 66-PEP-hhPPA	-0.05	-0.07	-0.08	-0.08	-0.06
$(\delta_{\text{HPEB}} - \delta_{\text{HhhPPA}})' (\text{MPa})^{1/2}$					
direct measurement	0.23	0.22	0.20	0.19	0.19
PEB-78-hhPPA; PEB-PEP-hhPPA	-0.07	-0.07	-0.07	-0.05	-0.03
c. Indirect Tentative Values of $\delta_{78} - \delta_{50\text{SPI}}$					
$(\delta_{\text{H78}} - \delta_{\text{H50SPI}})'$ or $(\delta_{\text{D78}} - \delta_{\text{D50SPI}})' (\text{MPa})^{1/2}$					
direct measurement <sup>a</sup>	~0	~0	~0	~0	~0
H78-D88-H50SPI	0.05	0.05	0.06	0.06	0.06
D78-H88-D50SPI	0.05	0.05	0.05	0.05	0.06
H78-DhhPPA-H50SPI	-0.03	-0.04	-0.04	-0.05	-0.05
D78-HhhPPA-D50SP	-0.00	-0.01	-0.00	-0.01	-0.01

<sup>a</sup> Values of  $\chi$  for 78/50SPI blends are very small but negative.

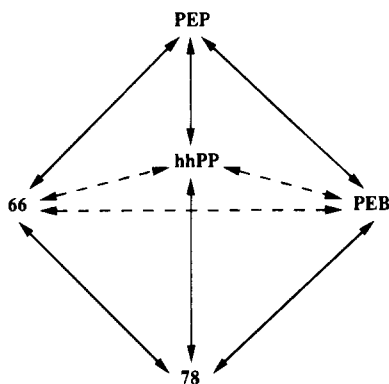


Figure 5. Diagram of interconnected blends for evaluating the mixing regularity of hhPP with other components. See text for an explanation of the solid and dashed lines.

and an internally consistent set of numerical values of  $\delta(T) - \delta_{97}(T)$  for HPEP, HPEB, and several HPB microstructures were assigned in previous work.<sup>7,8</sup> We use  $\delta_{\text{ref}}(T) = \delta_{97}(T)$  throughout.

In the course of assigning internally consistent values of  $\delta - \delta_{\text{ref}}$  for the PP, hhPP, 50SPI, and 75SPI microstructures, we found several new examples of irregular mixing, i.e., inconsistency with eq 2. Figure 5 is a diagram of the miscible blends of hhPP with various second components. The solid lines connect components when the ordering of  $\delta$  is clear. The dashed lines connect components for which the ordering is ambiguous because the label-switching effect is small (indicated by the question marks in Table 4, and in Table 3 of ref 5). The results of direct and indirect determinations of  $(\delta_{\text{PEP}} - \delta_{\text{hhPP}})'$ , shown in Table 5a, are typical. Direct tentative values were calculated from  $\chi$  for PEP/hhPP blends through eq 1. Indirect tentative values were obtained from their blends with intermediate components; e.g., a sum of direct tentative values,  $(\delta_{\text{HPEP}} - \delta_{\text{D66}})' + (\delta_{\text{D66}} - \delta_{\text{H78}})' + (\delta_{\text{H78}} - \delta_{\text{DhhPP}})'$ , gives an indirect tentative value for  $\delta_{\text{HPEP}} - \delta_{\text{DhhPP}}$ . The indirect estimates in Table 5a are in reasonable agreement at all temperatures (numerical consistency for all blends in each sequence other than the one involving hhPP itself had been established already<sup>8</sup>), but they differ somewhat

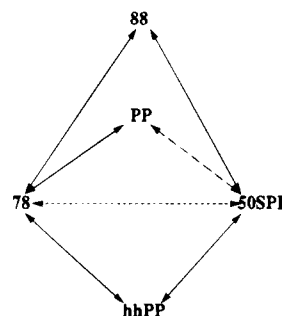


Figure 6. Diagram of interconnected blends used for assigning solubility parameters for the PP, hhPP, and 50SPI microstructures. See text for an explanation of solid, dashed, and dotted lines.

from the direct values—at low temperatures for HPEP/DhhPPA and at intermediate temperatures for the DPEP/HhhPPA—indicating that either PEP/hhPP or 78/hhPP or both mix irregularly.

More extreme discrepancies are found for 66/hhPP and PEB/hhPP blends (Table 5b). In both cases the direct tentative estimates are large and positive, while the indirect tentative estimates (the average for four sequences for each) are slightly negative. Similar discrepancies are found between the direct and indirect estimates for blends of PP with various second components.<sup>11</sup> However, blends of the connected pairs of components shown in Figure 6 appear to mix regularly. Again, the solid lines connect pairs with clear  $\delta$  ordering, while the dashed line connecting 50SPI and 78 reflects uncertainty in ordering. Blends of PP and 50SPI, indicated by the dotted line, have not been studied by SANS, but the critical temperatures for both D50SPI/HPBP and H50SPI/DPPB were estimated by light scattering.

The values of  $\chi$  for 50SPI/78 blends are very small at all temperatures (we ignore their negative signs), suggesting, in the absence of other information, that  $(\delta_{50\text{SPI}} - \delta_{78})'$  is essentially zero. The indirect tentative values from their blends with hhPP and from their blends with 88 (Table 5c) are also zero within the errors.<sup>8</sup> This agreement implies that hhPP/78, hhPP/50SPI, 88/78, and 88/50SPI as well as 78/50SPI mix regularly, i.e., in

**Table 6. Solubility Parameters from SANS Measurements Relative to an H97 Reference**

polymer	$(\delta - \delta_{\text{ref}})_{\text{SANS}}$ (MPa <sup>1/2</sup> ) at temp $T$ (°C)				
	27	51	83	121	167
H75SPI	-0.17	-0.17	-0.17	-0.16	-0.17
H97 <sup>a</sup>	0	0	0	0	0
H88 <sup>b</sup>	0.23	0.22	0.21	0.20	0.18
HPP	0.23	0.22	0.25	0.26	0.25
H50SPI	0.44	0.43	0.41	0.39	0.36
H78 <sup>a</sup>	0.49	0.48	0.46	0.44	0.41
HPEB <sup>a</sup>	0.72	0.72	0.71	0.69	0.66
H66 <sup>a</sup>	0.73	0.72	0.69	0.66	0.62
HhhPP	0.82	0.79	0.76	0.72	0.67
HPEP <sup>a</sup>	0.92	0.91	0.90	0.89	0.88

<sup>a</sup> Values assigned in ref 8. <sup>b</sup> Value assigned in ref 7.

**Table 7. Comparison of PVT-Based and SANS-Based Solubility Parameters Relative to an H97 Reference**

polymer	$(\delta - \delta_{\text{ref}})$ (MPa <sup>1/2</sup> ) at temp $T$					
	27 °C		83 °C		167 °C	
	PVT	SANS	PVT	SANS	PVT	SANS
HPP	0.2 <sub>0</sub>	0.23	0.1 <sub>7</sub>	0.25	0.0 <sub>1</sub>	0.25
H50SPI	0.4 <sub>5</sub>	0.44	0.3 <sub>8</sub>	0.41	0.6 <sub>8</sub>	0.36
HhhPP	0.6 <sub>3</sub>	0.82	0.7 <sub>7</sub>	0.76	0.8 <sub>2</sub>	0.67

a manner consistent with solubility parameter uniqueness. (We disregard as unlikely the alternative interpretation that some members of both groups of three blends mix irregularly but in such a manner as to produce apparent consistency at all temperatures.) Thus, confirmed values of  $\delta_{\text{hhPP}} - \delta_{78}$  and  $\delta_{50\text{SPI}} - \delta_{78}$  are obtained, which can then be translated to the  $\delta_{97}$  reference scale with  $\delta_{78} - \delta_{97}$  from ref 8. (Mixing regularity for 78/97 is supported by results in ref 1.) The values so obtained for  $\delta_{\text{hhPP}} - \delta_{\text{ref}}$  and  $\delta_{50\text{SPI}} - \delta_{\text{ref}}$  are given in Table 6.

The analysis to obtain internally consistent values for PP is similar but now based on comparing critical temperatures for PP/50SPI blends with those predicted by Flory-Huggins theory with the direct tentative values for  $\delta_{\text{PP}} - \delta_{78}$  (from  $\chi_{\text{PP/78}}$  via eq 1) and the now-assigned values of  $\delta_{78} - \delta_{50\text{SPI}}$ . Observed and predicted  $T_c$  are  $127 \pm 8$  and  $100$  °C for H50SPI/DPPB and  $95 \pm 10$  and  $60$  °C for D50SPI/HPPB. The agreement in both cases is within the experimental uncertainties of  $\chi(T)$ , thus providing evidence for regularity of mixing in PP/78 blends. The resulting values of  $\delta_{\text{PP}} - \delta_{\text{ref}}$  are given in Table 6.

SANS data are available for only two blends of 75SPI-75SPI/97B (both labeling configurations) and D75SPI/HPPA. The label-switching effect for 75SPI/97 suggests  $\delta_{97} > \delta_{75\text{SPI}}$ , but the effect in this case is really too small to be sure. However, the large  $\chi$  for D75SPI/HPPA and the observed immiscibility of 75SPI/88 blends up to at least  $140$  °C<sup>12</sup> both in fact supporting that ordering. Having no other recourse, we assumed that 75SPI and 97 mix regularly and used the inferred ordering to assign the values of  $\delta_{75\text{SPI}} - \delta_{\text{ref}}$  in Table 6. The values of  $(\delta_{\text{HPPA}} - \delta_{\text{D75SPI}})$  turned out to be in excellent agreement with the predictions of  $(\delta_{\text{PP}} - \delta_{\text{ref}})_{\text{SANS}}$  and  $(\delta_{75\text{SPI}} - \delta_{\text{ref}})_{\text{SANS}}$  in Table 6.

**C. Solubility Parameters from PVT Data.** The values of  $\delta - \delta_{\text{ref}}$  in Table 6 were assigned from SANS results on blends without regard for considerations beyond their ability to describe the interactions in a subset that conform with our definition of regular mixing. They are strictly empirical, having been obtained without appeal to any special molecular significance. The theory that underlies the solubility param-

eter formalism, however, associates  $\delta$  with the positive square root of the cohesive energy density of the pure liquid.<sup>9</sup> The cohesive energy density of a nonpolar liquid is related approximately to its internal pressure, which can be obtained from PVT measurements. This leads at low pressure to<sup>15</sup>

$$\delta_{\text{PVT}} = (T\alpha/\beta)^{1/2} \quad (6)$$

where  $\alpha$  is the thermal expansion coefficient of the liquid and  $\beta$  its isothermal compressibility. The values so obtained for HPP, HhhPP, and H50SPI are listed in Table 2. These PVT-based estimates relative to  $(\delta_{97})_{\text{PVT}}$ <sup>7,8</sup> are compared at three temperatures in Table 7 with the SANS-based results for HPP, HhhPP, and H50SPI from Table 6. Considering the large experimental uncertainties in  $(\delta - \delta_{\text{ref}})_{\text{PVT}}$ , we regard the overall agreement as reasonable and also consistent with the close parallels between  $(\delta - \delta_{\text{ref}})_{\text{SANS}}$  and  $(\delta - \delta_{\text{ref}})_{\text{PVT}}$  found earlier<sup>7,8</sup> for other components. The ordering of values for HPP, HhhPP, and H50SPI is the same by both methods, although there are numerical differences in some cases that may be beyond the error bars. The parallels offer additional support for our method of selecting out those blends that mix in a regular fashion.

**D. Effect of Segment Length.** Bates et al.<sup>16</sup> have noted a correlation between the phase behavior of diblocks and blends and the difference in the statistical segment length of the component species,  $\Delta l = |l_1 - l_2|$ . From this they infer the existence of a repulsive interaction, entropic in nature, that increases with  $\Delta l$  and arises from the conformational adjustments required to mix chains having different local length scales. They suggest the possibility that this "packing" contribution  $\Delta\chi$  dominates the observed  $\chi$  when the underlying interactions are weak, i.e., for nearly athermal blends, and could thereby explain the phase behavior-length mismatch correlation. A theory by Liu and Fredrickson,<sup>17</sup> based on the quite different mechanism of local nematic interaction, suggested the form

$$\Delta\chi = v_0 C (\Delta l/l)^2 \quad (7)$$

where  $\bar{l}$  is  $(l_1 + l_2)/2$  and  $C \sim 1/\bar{l}^3$ . Schweizer has raised strong objections to the nematic mechanism.<sup>18</sup> On the other hand, a recent theory of the conformational adjustment contribution<sup>19</sup> does not invoke that mechanism but leads, after some rearrangement, to the same form, with  $C = C_{\text{ca}} \sim (1/6\pi^2)(l_1 l_2)^{3/2}/(\bar{l}^2/\bar{l}^2)^2$  for midrange compositions ( $\phi \sim 0.5$ ) and for the suggested cutoff distance  $\Lambda_b^{-1} \sim (l_1 l_2)^{1/2}$ .

In an earlier study<sup>8</sup> we compared the values of  $\chi$  for the previous set of blends with estimates of  $\Delta\chi$  based on eq 7 and  $C = 1/\bar{l}^3$ . Component segment lengths were defined in terms of a common reference volume,<sup>16</sup>  $v_{\text{ref}} = 100 \text{ Å}^3$  for all components and temperatures in our case,

$$l_i(T) = \left[ \frac{6v_{\text{ref}} R_g^2(T)}{Nv(T)} \right]^{1/2} \quad (8)$$

a definition that is also consistent with the stipulation that  $\Delta\chi$  is governed by differences in the Helfand-Sapse packing parameter.<sup>19</sup> With  $\chi$  and  $\Delta\chi$  expressed in terms of the common reference volume  $v_{\text{ref}}$  we examined the magnitudes and trends of  $\chi$  and  $\Delta\chi$  with length-mismatch and temperature for a total of 15 pair combinations.<sup>8</sup> In order of magnitude and trend with

**Table 8. Component Statistical Segment Lengths Referred to a Fixed Lattice Size**

sample	$l$ (Å) at $T$ (°C)				
	27	51	83	121	167
H97B	5.0 <sub>2</sub>	4.9 <sub>9</sub>	4.9 <sub>8</sub>	4.9 <sub>6</sub>	4.9 <sub>2</sub>
H88	5.6 <sub>9</sub>	5.6 <sub>8</sub>	5.6 <sub>4</sub>	5.5 <sub>9</sub>	5.5 <sub>8</sub>
H78	5.7 <sub>6</sub>	5.7 <sub>4</sub>	5.7 <sub>4</sub>	5.7 <sub>6</sub>	5.7 <sub>4</sub>
H66	6.4 <sub>4</sub>	6.3 <sub>7</sub>	6.3 <sub>1</sub>	6.2 <sub>5</sub>	6.1 <sub>5</sub>
HPEB	6.1 <sub>3</sub>	5.9 <sub>7</sub>	5.9 <sub>0</sub>	5.8 <sub>3</sub>	5.7 <sub>4</sub>
HPEP	6.8 <sub>4</sub>	6.7 <sub>2</sub>	6.5 <sub>9</sub>	6.4 <sub>5</sub>	6.2 <sub>9</sub>
H50SPI	5.7 <sub>6</sub>	5.6 <sub>7</sub>	5.6 <sub>0</sub>	5.5 <sub>6</sub>	5.4 <sub>4</sub>
H75SPI	4.9 <sub>8</sub>	4.9 <sub>6</sub>	5.0 <sub>1</sub>	5.0 <sub>4</sub>	5.1 <sub>5</sub>
HhhPPA	5.9 <sub>8</sub>	6.0 <sub>0</sub>	5.9 <sub>4</sub>	5.8 <sub>6</sub>	5.7 <sub>9</sub>
HhhPPB	6.0 <sub>4</sub>	6.0 <sub>0</sub>	5.9 <sub>1</sub>	5.8 <sub>3</sub>	5.7 <sub>6</sub>
HhhPPC	5.9 <sub>7</sub>	5.9 <sub>2</sub>	5.8 <sub>3</sub>	5.7 <sub>6</sub>	5.7 <sub>0</sub>
HPPA	5.8 <sub>6</sub>	5.6 <sub>7</sub>	5.5 <sub>6</sub>	5.4 <sub>6</sub>	
HPPB	5.7 <sub>1</sub>	5.5 <sub>8</sub>	5.6 <sub>4</sub>	5.5 <sub>8</sub>	5.5 <sub>1</sub>

mismatch the parallels were reasonable: the calculated values of  $\Delta\chi$  ranged from  $10^{-4}$  to  $10^{-2}$ , and larger values were found in most cases when  $\chi$  was also large. The trends with temperature, however, were quite different. The variation of  $\Delta\chi$  with temperature, arising from differences in the temperature dependence of segment length, was found to bear little resemblance to the observed  $\chi$  vs  $T$  behavior.

The values of  $\Delta\chi$  obtained from eq 7 and  $C = C_{ca}$  are smaller than those with  $C = 1/\bar{l}^3$  by nearly 2 orders of magnitude. Thus, the estimates in this case range from  $10^{-4}$  to  $10^{-6}$ , suggesting that the contribution to  $\chi$  from conformational adjustment<sup>19</sup> is negligible. The predicted values of  $\Delta\chi$  can in fact be forced into the observed range for  $\chi$  with a smaller cutoff distance,  $\Lambda_b^{-1} \sim 0.25 (l_1 l_2)^{1/2}$ , but that is certainly arbitrary and would appear to place the cutoff well inside the segment length itself. Nevertheless, it still seemed worthwhile to compare the trends predicted by eq 7 with the results for the 13 new microstructural pairings presented here. Values of  $l$  were calculated with eq 8 and the data in Tables 1 and 2b. They are listed in Table 8. The values of  $\chi$  in Table 4 were also converted to  $v_{ref}$ .

What we find is that now even the trends with mismatch are erratic. Thus, at 83 °C, for example,  $\Delta l/\bar{l}$  is small for both 78/50SPI ( $\sim 0.03$ ) and PP/hhPP ( $\sim 0.05$ ), yet  $\chi$  is small for 78/50SPI ( $\sim 0$ ) but large for PP/hhPP ( $\sim 15 \times 10^{-4}$ ). Also,  $\Delta l/\bar{l}$  is large for both PP/PEP ( $\sim 0.16$ ) and hhPP/PEP ( $\sim 0.11$ ), yet  $\chi$  is large for PP/PEP ( $\sim 30 \times 10^{-4}$ ) but small for hhPP/PEP ( $\sim 6 \times 10^{-4}$ ).

The predicted trends with temperature are also inconsistent:

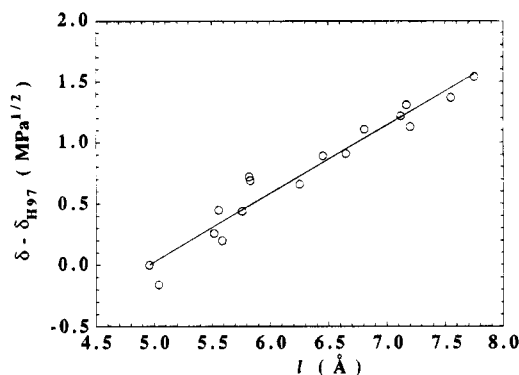
(a) For PP/hhPP,  $\Delta l/\bar{l}$  is nearly independent of temperature, yet  $\chi$  decreases fairly rapidly with increasing temperature (Figure 2).

(b) For PEP/hhPP,  $\Delta l/\bar{l}$  decreases monotonically with temperature, yet  $\chi$  first decreases and then increases with temperature (Figure 3).

(c) For PEP/PP,  $\Delta l/\bar{l}$  decreases with temperature, yet  $\chi$  increases with temperature (Figure 4). All three of these blends mix irregularly (see below), so the assigned solubility parameters also fail to predict the trends in those cases. For others, however, the solubility parameter prediction for  $\chi$  vs  $T$  is quite satisfactory, but  $\Delta l/\bar{l}$  still does not capture the trends. Thus:

(d) For 78/50SPI,  $\Delta l/\bar{l}$  increases with temperature, yet  $\chi$  is independent of temperature (Figure 1).

(e) The temperature dependence of  $l$  is nearly the same for 66 and PEB, yet  $\chi$  for their blends with 52, PEP, and 78 have very different temperature dependences (see Figure 1 in ref 8 for the PEP/66–PEP/PEB, 52/66–52/PEB, and 78/66–78/PEB comparisons).

**Figure 7.** Confirmed values of relative solubility parameters for SANS as a function of statistical segment length for several microstructures.

Accordingly, by the criteria we have examined—order of magnitude, trend with mismatch, trend with temperature—the current theories of packing contributions do not provide a unifying principle for describing the interactions in blends of saturated hydrocarbon polymers. The conformational adjustment contribution appears to be too small. Beyond that, however, the temperature trends it predicts are seldom consistent with the experimental data. The predicted trends with segment length mismatch are also erratic, being broadly consistent with experiment in some cases but inconsistent in others. Finally, we are inclined for still another reason to doubt that interaction strengths in blends of saturated hydrocarbon polymers are strongly affected by conformational adjustment. Deuterium labeling should have a negligible influence on mutual packing requirements, since the molecular shapes are so little changed. It is therefore difficult to reconcile the significant change in  $\chi$  produced by merely switching the labels from one component to the other<sup>3–5</sup> with an interaction strength that is dominated by conformational adjustment.

Lacking compelling evidence to the contrary, it seems preferable at this point to maintain the conventional stance: the interactions between saturated hydrocarbons are primarily enthalpic. In our view, the temperature dependence of  $\chi$  simply reflects a relative variation with temperature in the various underlying energies.

Nevertheless, there is still an overall tendency that is certainly as was first suggested by Bates et al.:<sup>16</sup> there does appear to be some connection between phase behavior and  $\Delta l/\bar{l}$  within broad component families such as the saturated hydrocarbon polymers. Indeed, there is a strong parallel between the segment length of a component and what we have termed its *regular mixing* characteristics. Figure 7 shows the relationship between  $l$  and  $(\delta - \delta_{ref})_{SANS}$  for the total of 17 saturated hydrocarbon polymers that we have studied thus far. The results for 121 °C are shown, but the relationship at other temperatures is similar. The statistical segment length of a component correlates linearly with the parameter that specifies its regular mixing behavior with the other components. The least-squares line in Figure 7 (correlation coefficient 0.97) is

$$(\delta - \delta_{ref})_{SANS} = 0.56l - 2.77 \quad (9)$$

when  $(\delta - \delta_{ref})_{SANS}$  and  $l$  are expressed in units of  $\text{MPa}^{1/2}$  and Å. This translates to an expression of the same form as eq 7 for the interaction parameters at 121 °C in regular mixtures (eq 1,  $v_{ref} = 100$  Å):



$$\chi = 0.21(\Delta l/\bar{l})^2 \quad (10)$$

in which we have used 6 Å as a representative value for  $\bar{l}$ . It is important to note, however, that the scatter around the line in Figure 7 is much larger than the uncertainties in the individual values, which are no larger than  $\pm 0.08 \text{ MPa}^{1/2}$  (and usually  $\pm 0.03 \text{ MPa}^{1/2}$ ) for the  $(\delta - \delta_{\text{ref}})_{\text{SANS}}$  assignments and  $\pm 0.1 \text{ Å}$  for  $l$ . The line represents only an overall trend for saturated hydrocarbon polymers: component individuality still modulates in a very significant way this globally linear correlation between  $(\delta - \delta_{\text{ref}})_{\text{SANS}}$  and  $l$ . When applied to individual blends that mix regularly, for which  $|\delta_2 - \delta_1|$  must be smaller than  $0.3 \text{ MPa}^{1/2}$  ( $\chi \leq 20 \times 10^{-4}$ ) at  $N \sim 10^3$  ( $M \sim 70\,000$ ) in order to produce miscibility, the modulations in Figure 7 clearly dominate, and the uncritical use of eq 10 leads to serious errors, as the previous comparisons make clear.

Figure 7 and eq 9 also imply a global correlation between segment length and the *PVT* properties of saturated hydrocarbon polymers. Thus, in this and past work we have shown that  $(\delta - \delta_{\text{ref}})_{\text{PVT}}$  and  $(\delta - \delta_{\text{ref}})_{\text{SANS}}$  are closely related, so a linear correlation between  $(\delta - \delta_{\text{ref}})_{\text{PVT}}$  and  $l$  is also to be expected. We examine this and other questions on the relationship of regular and irregular mixing to pure-component *PVT* properties in a forthcoming paper.<sup>20</sup>

**E. Irregular Mixing.** Consistency with the solubility parameter formalism was demonstrated earlier for 9 of 10 cross-checked pairs of microstructures;<sup>8</sup> the only clear exception in that group was the 66/PEB pair. Six additional exceptions were identified among the 13 pairs in the present study—hhPP with PEP, PEB, 66, and PP; PP with PEP and 97—giving, in all, 16 pairs that mix regularly and 7 that mix irregularly. Irregularity can be expressed in terms of an extra free energy density  $X_E \phi_1 \phi_2$ , which we define such that

$$X_E = \chi k_B T / v_0 - (\delta_2 - \delta_1)^2 \quad (11)$$

Accordingly,  $X_E$  is zero if the interaction density is equal, within the errors, to the value predicted from independently assigned and verified solubility parameters. Values of  $X_E$  were calculated through eq 11 with  $\chi$  for the 7 blends that mix irregularly and the assigned solubility parameters for their components (Table 7). The results are plotted in Figures 8–10.

The smallest  $X_E$  values for blends that mix irregularly are found for the 66/PEB and PEP/hhPP pairs. They are shown in Figure 8 along with the average spread of values,  $\pm 0.32 \times 10^{-2} \text{ MPa}$ , obtained for the 16 pairs that mix regularly. Relative to the other irregular mixtures, the 66/PEB and PEP/hhPP results extend only slightly beyond the “regularly mixed” range. The 66/PEB values are fairly firm, having been established earlier<sup>8</sup> with many cross-checks. The values and particularly the crossover in sign for PEP/hhPP are barely significant within the greater uncertainties of the hhPP assignment made here. The values of  $X_E$  for PEB/hhPP, 66/hhPP, and PP/97 (Figure 9) are positive and clearly beyond the regularly mixed range. The 66/hhPP pair appear to mix regularly at elevated temperatures ( $T > 100^\circ\text{C}$ ). The values for PP/97 at low temperatures are also positive and still larger, although again their mixing appears to approach regularity at elevated temperatures.

Positive deviations from regular mixing, such as shown for the most part in Figures 8 and 9, are broadly

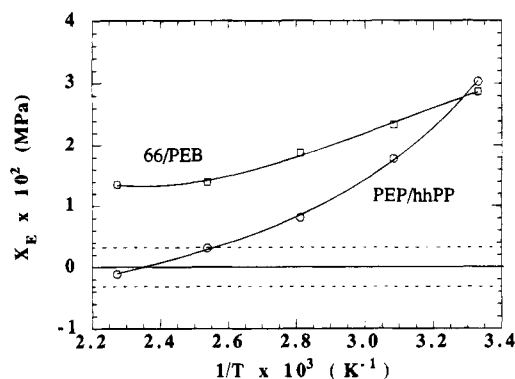


**Figure 8.** Coefficients of extra free energy density associated with mixing irregularity in 66/PEB and PEP/hhPP blends. The dashed lines indicate the average for blends that mix regularly.

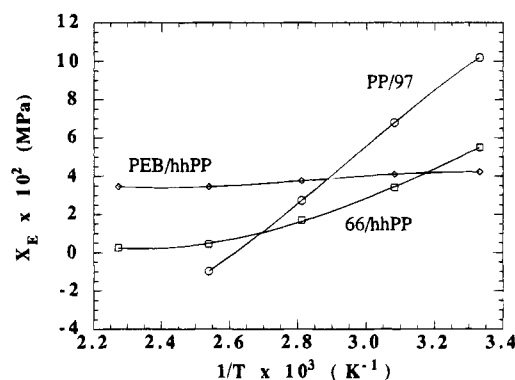


**Figure 9.** Coefficient of extra free energy density associated with mixing irregularity in PEB/hhPP, 66/hhPP, and PP/97 blends.

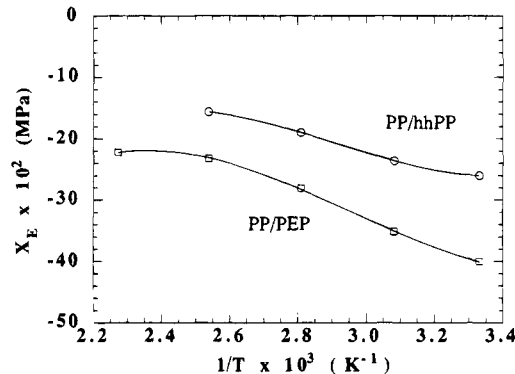


**Figure 10.** Coefficient of extra free energy density associated with mixing irregularity in PP/hhPP and PP/PEP blends.

consistent with equation-of-state theory,<sup>21</sup> but the observed trend with temperature is unexpected. Thus,  $X_E$  decreases with increasing temperature and, except for PEB/hhPP, becomes zero within the errors at the highest temperatures investigated. Equation-of-state contributions, however, are expected to increase with increasing temperature, being the result of diverging free-volume requirements for the individual components that leads eventually to an LCST. The behavior of PEP/hhPP, which indicates an UCST–LCST phase diagram (Figure 3), seems especially counterintuitive. Thus, its high-temperature behavior is dominated by solubility parameter differences ( $X_E \sim 0$ ), which grow larger with increasing temperature and suggest an eventual LCST. Its behavior at lower temperatures, on the other hand, is increasingly influenced by  $X_E$ , which grows rapidly enough with decreasing temperature to suggest an eventual UCST.



In contrast with the positive deviations from regularity shown in Figures 8 and 9, destabilizing those blends and favoring phase separation, the deviations for PP/hhPP and PP/PEP blends, shown in Figure 10, are negative and relatively large. In both cases  $X_E$  strongly dominates the interactions, and irregularity massively favors miscibility. Thus, for example, at 83 °C  $\chi_{PP/PEP}$  is  $47 \times 10^{-4}$  (Table 4), while the value calculated with the assigned solubility parameters (Table 6) is  $130 \times 10^{-4}$ . The corresponding observed and calculated  $\chi_{PP/hhPP}$  are  $26 \times 10^{-4}$  and  $87 \times 10^{-4}$ , respectively. Such behavior resembles closely the single phase stabilization of 100/PEP (PEE-PEP) and 08/100 (PE-PEE) diblocks<sup>16</sup> relative to expectations based on solubility parameter assignments.<sup>8</sup> We have found examples of even stronger stabilization in certain blends of polyisobutylene,<sup>12,22</sup> such that the interaction parameter itself is negative and very large. Negative deviations from regularity seemingly cannot be reconciled by free volume theories.<sup>21</sup>

Irregular mixing of liquids, i.e., departures in interaction strength from values based on preassigned and carefully verified solubility parameters, can appear for many reasons, whether the components are monomeric or polymeric, and has been expressed in many ways.<sup>23</sup> Thus, for example, in regular solution theory the interaction strength of a blend is proportional to the net energy change per pair contact,  $\Delta u = \epsilon_{12} - (\epsilon_{11} + \epsilon_{22})/2$ , where the  $\epsilon_{ij}$  are all negative. Berthelot's conjecture,<sup>23</sup>  $\epsilon_{12} = -(\epsilon_{11}\epsilon_{22})^{1/2}$ , takes that immediately to the perfect square form, such that  $\chi \propto [(-\epsilon_{11})^{1/2} - (-\epsilon_{22})^{1/2}]^2$  as required by the Hildebrand formulation (eq 1). But beyond an exact result for dielectric spheres,<sup>9</sup> the conjecture remains theoretically unsupported and thus technically suspect for anything as complicated as liquid mixtures of real molecules, even saturated hydrocarbons. On the other hand,  $\epsilon_{12} = -(\epsilon_{11}\epsilon_{22})^{1/2}$  cannot be outlandishly wrong, since solubility parameter ideas have been used successfully for many years as guides for estimating the mutual solubility of small-molecule liquids.<sup>9,24</sup>

One way to parametrize the departures from regular mixing is simply to apply an earlier conjecture about the cross-term,<sup>23</sup>  $\epsilon_{12} = -\lambda(\epsilon_{11}\epsilon_{22})^{1/2}$ , in which  $\lambda$  is adjustable and  $\lambda = 1$  corresponding to regularity. When translated to the language of solubility parameters, the generalized cross-term leads to

$$X_E = 2(\lambda - 1)\delta_1\delta_2 \quad (12)$$

Only differences in solubility parameters are obtainable from SANS, but the PVT measurements provide what are probably reasonable estimates of the absolute values. For the pair with the largest irregularity, PP/PEP,  $X_E$  is roughly  $-0.3$  MPa (Figure 10) at intermediate temperatures,  $\delta_{PP} = 16.9$  MPa<sup>1/2</sup> (Table 2,  $T \sim 100$  °C), and  $\delta_{PEP} = 17.1$  MPa<sup>1/2</sup> (Table 3,  $T \sim 100$  °C in ref 8). Taken together with eq 12, these values give  $\lambda = 0.9995$ . Thus, even in the most extreme example of irregularity represented here, the apparent departure from Berthelot's conjecture is remarkably small. Indeed, considerably the exquisite balance in energies required, it is a wonder that the solubility parameter formalism works for any of our blends. For mixtures of small molecules, where the solubility parameter difference near phase boundaries is of course much greater, the departures from regularity are larger but usually in the same direction ( $\lambda < 1$ ).<sup>23</sup>

Although the sample size is small, it is curious that small departures from regularity tend to be positive (within the uncertainties), while larger departures (PP/PEP, PP/hhPP, PEP/100, 08/100, and the polyisobutylene blends) tend to be negative. Some parallels between the departures and the more detailed nature of component PVT behavior will be described in a later publication.<sup>20</sup>

## Concluding Remarks

The thermodynamic interactions obtained for the blends studied over the full course of our work fall into three categories:

(A) The consistency of the blend interactions with the solubility parameter formulation has been confirmed by one or more cross-checks, with results used to establish a table of component solubility parameters relative to  $\delta_{97}$ .

(B) The consistency of the blend interactions with the solubility parameter formulation is less sure because cross-checks were lacking or less direct, with results used to fill in the table when no other route for a component was available. (75SPI and some of the HPB assignments in ref 7.)

(C) The inconsistency of the blend interactions with the solubility parameter formulation is confirmed by cross-checks, with results expressed in terms of  $X_E$ , the extra free energy density coefficient for the blend relative to the solubility parameter prediction. (The seven irregular blends identified here.)

The bounds of these categories are blurred. The 38/PEP and 52/PEB blends<sup>8</sup> are classified A, but their values of  $X_E$ , which average to  $-0.77 \times 10^{-2}$  and  $+0.76 \times 10^{-2}$  MPa, respectively, are somewhat beyond the  $\pm 0.32 \times 10^{-2}$  MPa average for all category A blends and might just as well have qualified them for category C. Most of this blurring is within the experimental uncertainties in  $\chi$ ,<sup>8</sup> but the magnitudes of mixing irregularity probably take on a continuum of values with some that are inevitably marginal.

The boundary between categories A and B is also blurred, depending on the criterion for confirmation. Thus, confirmation of  $\delta_{78} - \delta_{97}$  rests on the agreement between the tentative indirect value,  $(\delta_{78} - \delta_{88})' + (\delta_{88} - \delta_{97})'$ , and semiquantitative inferences from the two-phase SANS scattering of 78/97 blends at elevated temperature.<sup>1</sup> The assignments for both  $\delta_{75SPI} - \delta_{ref}$  and  $\delta_{PP} - \delta_{ref}$  are at least partially verified by the agreement between the direct tentative  $(\delta_{D75SPI} - \delta_{HPPA})'$  and the result calculated with the independently assigned  $\delta_{75SPI} - \delta_{ref}$  and  $\delta_{PP} - \delta_{ref}$ . Also, mixing regularity of HPB blends from 00 (linear polyethylene) to 35 is inferred mainly from their agreements with the copolymer equation over that limited range.<sup>5</sup> The values for those species, however, are also linked with  $\delta_{52}$  and hence with the others by consistent indirect values for  $(\delta_{08} - \delta_{52})'$  and  $(\delta_{00} - \delta_{52})'$ , as obtained through sequences that contain different HPB components (see Appendix B).

We have reviewed the data on the temperature dependence of  $\chi$  for all blends to see if there is any correspondence between the multitude of observed  $\chi$ -( $T$ ) shapes and either segment length mismatch  $\Delta l/l$  or mixing irregularity  $X_E$ . The form  $A/T + B$  is found for many blends, but both large and small  $\Delta l/l$  as well as large and small  $X_E$  are represented. Among the others, where  $\chi$  vs  $1/T$  is curved in various ways, the same is true: large and small values of both  $\Delta l/l$  and  $X_E$  appear

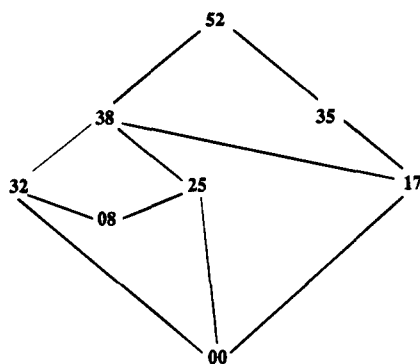


**Figure 11.** Diagram of interconnected blends for evaluating mixing regularity among model ethylene-butene copolymer species.

to be represented more-or-less at random. The shape of  $\chi(T)$  for a blend appears to be uncorrelated with  $\Delta l/l$  and  $X_E$ .

Finally, the values of  $\delta$  from both SANS and PVT data have temperature dependences that vary with microstructure. Accordingly, the temperature dependence of  $\chi$  for any particular blend would appear to contain little direct information about the nature of the mixing process itself or the mechanisms for interaction that favor or retard it. Moreover, for the many blends that we have classified as regular in mixing, we find no evidence suggesting that the interactions between components that govern mixing are other than purely enthalpic in origin.

**Acknowledgment.** Financial support (W.W.G., R.K., and G.C.R.) was provided by grants from the National Science Foundation to Princeton University (DMR89-05187 and DMR93-10762). We are grateful to Greg Dee for the PVT measurements and to him as well as Frank Bates, Glenn Fredrickson, and Andrea Liu for stimulating discussions. In addition, we thank Ken Schweizer for comments on various aspects of our results and particularly for pointing out to us the relevance of label-switching effects to the issue of conformational adjustment contributions.

#### Appendix A. Molecular Weight Dependence of the Interaction Strength

According to Flory-Huggins theory, the interaction parameter depends on temperature and the component microstructures alone:  $\chi$  should be independent of the component concentrations ( $\phi_1$ ,  $\phi_2$ ) and chain lengths ( $N_1$ ,  $N_2$ ). As documented elsewhere,<sup>6</sup> we typically observe a mild  $\phi$  dependence, roughly symmetrical about a rather flat minimum in the midrange ( $\phi_1 \sim \phi_2 \sim 0.5$ ). (This effect may well account for the modest difference in  $\chi$  for DPEP/HPPA blends at  $\phi_{PP} = 0.70$  and  $0.87$  (Table 4).) Over the full course of our investigations we have obtained results which suggest that  $\chi$  is insensitive to  $N_1$  and  $N_2$ . Thus, among blends of HPB components, 97A/88 and 97B/88 blends have the same  $\chi$ , within the errors ( $\sim \pm 1.5 \times 10^{-4}$ ) although  $N$  for 97A and 97B differ by nearly a factor of 2.<sup>1</sup> Also,  $\chi$  for various blends of linear polyethylene fractions SRM-1482, -1483, -1484 with D17, D25, and D32 correlate well through the copolymer equation (as expected over this limited composition range<sup>7</sup>) despite differences of nearly a factor of 9 in  $N$  for the polyethylenes.<sup>5</sup>

These inferences of  $N$  independence are supported here (see Table 4) by data for blends of DhhPPA and DhhPPB with H66 and also for blends of HhhPPA and

HhhPPB with DPEB. In both cases,  $\chi$  is the same, well within the errors, and the two hhPP samples differ in  $N$  by about a factor of 3. Among all our results, the only apparent counterexample is PEP/hhPP (see Table 4). Blends of DPEP with HhhPPB ( $N = 910$ ) and HhhPPC ( $N = 2050$ ) have the same  $\chi$  at each temperature within the errors, but the values for DPEP with HhhPPA ( $N = 320$ ) are much smaller. The fractional contribution of interactions to the coherent SANS intensity is small and highly uncertain for the DPEP/HhhPPA blend (see ref 1 for a discussion of errors in  $\chi$ ). However,  $\chi$  for HPEP/DhhPPA is also significantly smaller than  $\chi$  for HPEP/DhhPPC, where the interactions are larger and less uncertain. Thus, there appears to be a chain length dependence in the PEP/hhPP interactions, but there is still enough uncertainty that we intend to make a more thorough examination of  $\chi$  for PEP/hhPP blends in the future. Until then, we use the results for PEP/hhPPC blends in any numerical assignments of interaction strengths.

#### Appendix B. Self-Consistency of Solubility Parameter Assignments for Ethylene-Butene Copolymers (Ethylene-Rich Range)

We have established the self-consistency of the assigned solubility parameters for the high butene content ( $38 \leq y \leq 97$ ) ethylene-butene (saturated polybutadienes) in previous publications.<sup>7,8</sup> Here we evaluate the self-consistency of the assignments for the high ethylene content ( $0 \leq y \leq 52$ ) HPB structures examined.

We have examined eight materials with butene content ranging from 0 to 52 wt % and assigned relative solubility parameters as a function of temperature. The various series of interconnected blends examined are pictorially represented in Figure 11. Using these series, we estimate the values of  $\delta_{08} - \delta_{52}$  and  $\delta_{00} - \delta_{52}$ . The assignments were made only at 167 °C. Below this temperature, data in several cases could not be acquired due to crystallization or phase separation. The indirect values shown below agree well with those inferred previously.<sup>7,8</sup>

$$\text{H52/D38-D38/H32-H32/D08} \quad \delta_{D08} - \delta_{H52} = 0.55$$

$$\text{H52/D38-D38/H25-H25/D08} \quad \delta_{D08} - \delta_{H52} = 0.56$$

$$\text{D52/H38-H38/D32-D32/H08}^a \quad \delta_{H08} - \delta_{D52} = (>0.52)$$

$$\text{D52/H38-H38/D25-D25/H08} \quad \delta_{H08} - \delta_{D52} = 0.58$$

$$\text{D52/H38-H38/D32-D32/H00} \quad \delta_{H00} - \delta_{D52} = 0.64$$

$$\text{D52/H38-H38/D25-D25/H00} \quad \delta_{H00} - \delta_{D52} = 0.63$$

$$\text{D52/H38-H38/D17-D17/H00}^b \quad \delta_{H00} - \delta_{D52} \approx 0.62$$

$$\text{D52/H35-H35/D17-D17/H00}^b \quad \delta_{H00} - \delta_{D52} \approx 0.61$$

<sup>a</sup> D32/H08 phase separated at 167 °C. Estimated by extrapolation from higher temperatures. <sup>b</sup> D17/H00

phase separated at 167 °C. Estimated by extrapolation from higher temperatures.

## References and Notes

- (1) Balsara, N. P.; Fetters, L. J.; Hadjichristidis, N.; Lohse, D. J.; Han, C. C.; Graessley, W. W.; Krishnamoorti, R. *Macromolecules* **1992**, *25*, 6137.
- (2) Walsh, D. J.; Graessley, W. W.; Datta, S.; Lohse, D. J.; Fetters, L. J. *Macromolecules* **1992**, *25*, 5236.
- (3) Graessley, W. W.; Krishnamoorti, R.; Balsara, N. P.; Fetters, L. J.; Lohse, D. J.; Schulz, D. N.; Sissano, J. A. *Macromolecules* **1993**, *26*, 1137.
- (4) Balsara, N. P.; Lohse, D. J.; Graessley, W. W.; Krishnamoorti, R. *J. Chem. Phys.* **1994**, *100*, 3905.
- (5) Graessley, W. W.; Krishnamoorti, R.; Balsara, N. P.; Fetters, L. J.; Lohse, D. J.; Schulz, D. N.; Sissano, J. A. *Macromolecules* **1994**, *27*, 2574.
- (6) Krishnamoorti, R.; Graessley, W. W.; Balsara, N. P.; Lohse, D. J. *J. Chem. Phys.* **1994**, *100*, 3894.
- (7) Graessley, W. W.; Krishnamoorti, R.; Balsara, N. P.; Butera, R. J.; Fetters, L. J.; Lohse, D. J.; Schulz, D. N.; Sissano, J. A. *Macromolecules* **1994**, *27*, 3896.
- (8) Krishnamoorti, R.; Graessley, W. W.; Balsara, N. P.; Lohse, D. J. *Macromolecules* **1994**, *27*, 3073.
- (9) Hildebrand, J. H.; Scott, R. L. *The Solubility of Non-Electrolytes*, 3rd ed.; Van Nostrand-Reinhold: Princeton, NJ, 1950 (reprinted by Dover Publications: New York, 1964).
- (10) (a) Mays, J. W.; Hadjichristidis, N.; Fetters, L. J. *Macromolecules* **1984**, *17*, 2723. (b) Xu, Z.; Mays, J. W.; Chen, X.; Hadjichristidis, N.; Schilling, F.; Bair, H. E.; Pearson, D. S.; Fetters, L. J. *Macromolecules* **1985**, *18*, 2560. (c) Hattam, P.; Gauntlett, S.; Mays, J. W.; Hadjichristidis, N.; Young, R. N.; Fetters, L. J. *Macromolecules* **1991**, *24*, 6199.
- (11) Hammouda, B.; Krueger, S.; Glinka, C. J. *J. Res. Natl. Inst. Stand. Technol.* **1993**, *98*, 31.
- (12) Krishnamoorti, R. Doctoral Dissertation, Princeton University, 1994.
- (13) Values of  $\chi$  for PP/97 blends are given in Table 4. The H97 microstructure corresponds very closely with that of atactic poly(1-butene), which would be H100 in our terminology. Others have suggested that the isotactic and atactic versions of polypropylene and poly(1-butene) are at least partially miscible in the melt state, which our results tend to support: (a) Lee, M.-S.; Chen, S.-A. *J. Polym. Sci., Part C: Polym. Lett.* **1987**, *25*, 37. (b) Marand, H.; Chan, F. M.; Lee, T. H.; Mays, J. W. *Am. Chem. Soc. PMSE Prepr.* **1992**, *67*, 199.
- (14) Lohse, D. J.; Fetters, L. J.; Doyle, J. J.; Wang, H.-C.; Kow, C. *Macromolecules* **1993**, *26*, 3444.
- (15) (a) Allen, G.; Gee, G.; Wilson, G. J. *Polymer* **1960**, *1*, 456. (b) Allen, G.; Gee, G.; Mangaraj, D.; Sims, D.; Wilson, G. J. *Polymer* **1960**, *1*, 467.
- (16) Bates, F. S.; Schulz, M. F.; Rosedale, J. H.; Almdal, K. *Macromolecules* **1992**, *25*, 5547.
- (17) Liu, A. J.; Fredrickson, G. H. *Macromolecules* **1992**, *25*, 5551.
- (18) Schweizer, K. S. *Macromolecules* **1993**, *26*, 6050.
- (19) Fredrickson, G. H.; Liu, A. J.; Bates, F. S. *Macromolecules* **1994**, *27*, 2503.
- (20) Krishnamoorti, R.; Graessley, W. W.; Dee, G. T.; Walsh, D. J.; Fetters, L. J.; Lohse, D. J., manuscript in preparation.
- (21) Patterson, D.; Robard, A. *Macromolecules* **1978**, *11*, 690.
- (22) Krishnamoorti, R.; Graessley, W. W.; Fetters, L. J.; Garner, R. T.; Lohse, D. J. *Macromolecules*, in press.
- (23) Rowlinson, J. S.; Swinton, F. L. *Liquids and Liquid Mixtures*, 3rd ed.; Butterworths: London, 1982.
- (24) (a) Barton, A. F. M. *Handbook of Solubility Parameters and Other Adhesion Parameters*; CRC Press: Boca Raton, FL, 1983. (b) Coleman, M. M.; Graf, J. F.; Painter, P. C. *Specific Interactions and Miscibility of Polymer Blends*; Technomic: Lancaster, PA, 1991.

MA941206L